

Magnetization curves for anisotropic magnetic impurities adsorbed on a normal metal substrate

Rok Žitko

Jožef Stefan Institute, Jamova 39, SI-1000 Ljubljana, Slovenia rok.zitko@ijs.si

Abstract. Magnetization curves $\langle S_z \rangle(B, T)$ for magnetic impurities which couple to the host medium via exchange interactions are computed using the numerical renormalization group. Deviations from the ideal paramagnetic behavior (as described by the Brillouin function) is discussed for various T/T_K ratios, where T_K is the Kondo temperature, focusing on the implications for the interpretation of experimental X-ray magnetic circular dichroism (XMCD) results. The case of anisotropic impurities is also considered.

1.1 Introduction

A recent trend in the field of surface magnetism is to study magnetic properties of single adsorbed atoms on various surfaces [1]. Particularly interesting systems consist of magnetic impurities (transition metals, lanthanides) on noble metal surfaces where many-particle physics such as the Kondo effect [2] play an important role [3, 4]. In addition to low-temperature scanning tunneling microscopy (STM) which allows to probe the adsorbate electronic and magnetic properties at the level of single atoms [3, 5–8], a commonly applied technique is the X-ray magnetic circular dichroism (XMCD) [9–11]: the absorption coefficient $\mu(E)$ for X-rays with energy E is different in magnetic materials for right-circular and left-circular polarization [12, 13]. XMCD allows to identify the magnetization direction and strength, magnetocrystalline anisotropy, and magnitudes of the spin (S) and orbital (L) magnetic moments separately [14–16]. While XMCD does not allow to probe individual atoms, but provides sample-averaged results, it is nevertheless an element-selective technique which can be therefore used to study dilute concentrations of adsorbed atoms [10]. Since dilute magnetic impurities typically do not order magnetically, the experiments are performed by applying an external magnetic field and measuring the magnetization curves, $\langle S_z \rangle(B)$. By fitting the results using Brillouin or Langevin functions, the magnetic moments are then

extracted. Magnetic anisotropy effects may also be studied by applying the magnetic field in various spatial directions [15]. Recently, it has also been demonstrated that the magnetization curves can be measured using an STM with spin-polarized tip [7].

When the magnetic impurity couples to the host, the description in terms of ideal paramagnetic moment is not appropriate. In particular, the Kondo effect significantly modifies the magnetization curves and introduces a new energy scale T_K , the Kondo temperature, to the problem. These effects are most pronounced at low temperatures and magnetic fields, $T, B \ll T_K$. The purpose of the present work is to calculate the magnetization curves for simple impurity models using a numerically exact non-perturbative method (numerical renormalization group, NRG) in order to determine how the impurity-host coupling may manifest in experimental XMCD magnetization curves.

1.2 Kondo model

For simplicity, we first consider the pure-spin Kondo model. Two aspects of the full problem are therefore neglected: 1) all features related to orbital magnetism, and 2) the reduction of the moment due to the hybridization with the conduction-band electrons. This implies that the expectation value $\langle S^2 \rangle$ will always be equal to $S(S+1)$, irrespective of the strength of the exchange coupling of the impurity spin with the host material (i.e. charge fluctuations are fully neglected). While this is clearly an oversimplification of the full problem, the Kondo model is sufficient to study the main effects of the exchange coupling to the substrate electrons. The additional effects of the hybridization are considered later in Sec. 1.6.

We thus study the Kondo model as given by the following Hamiltonian [2]:

$$H = \sum_{k,\sigma} \epsilon_k c_{k\sigma}^\dagger c_{k\sigma} + J \mathbf{S} \cdot \mathbf{s} + g \mu_B \mathbf{S} \cdot \mathbf{B}, \quad (1.1)$$

where \mathbf{S} is the quantum-mechanical spin- S operator which describes the magnetic impurity, while \mathbf{s} is the spin-density of conduction-band electrons at the impurity position. The gyromagnetic ratio g is assumed to be isotropic, μ_B is the Bohr magneton and \mathbf{B} the external magnetic field. We assume a constant density of states, $\rho = 1/2W$, where W is the half-width of the conduction band (which is taken as the energy unit in the following). The strength of the exchange coupling is given by ρJ , in terms of which the Kondo temperature is given approximately as $T_K \approx D \sqrt{\rho J} \exp(-1/\rho J)$. For anisotropic impurities, we add an additional term to the Hamiltonian [5, 17, 18]:

$$H_{\text{aniso}} = D S_z^2 + E (S_x^2 - S_y^2). \quad (1.2)$$

Here D is the axial magnetic anisotropy and E the transverse magnetic anisotropy. By convention, the z axis is chosen so that $|D|$ is maximal, while

axes xy are rotated so that $E > 0$. If $D < 0$, the z -axis is an easy-axis; if $D > 0$, the anisotropy is planar.

For a decoupled impurity, the impurity is an ideal paramagnetic spin whose magnetization curve $\langle S_z \rangle = SB_S(x)$ is given exactly by the Brillouin function

$$B_S(x) = \frac{2S+1}{2S} \coth \left[\frac{2S+1}{2S} x \right] - \frac{1}{2S} \coth \left[\frac{1}{2S} x \right], \quad (1.3)$$

where $x = g\mu_B BS/k_B T$ is the rescaled magnetic field.

Experimentalists commonly extract parameters using a classical-spin approximation, taking an expression for the energy of the form [7, 10]

$$E = -mB \cos \theta - K \cos^2 \theta, \quad (1.4)$$

where B is taken as the z axis, θ is the angle between the field and the magnetic moment, and K is the magnetic anisotropy energy. The magnetization is then given by

$$M = M_{\text{sat}} \frac{\int d\phi d(\cos \theta) \cos \theta e^{-E/k_B T}}{\int d\phi d(\cos \theta) e^{-E/k_B T}}, \quad (1.5)$$

where M_{sat} is the saturation magnetization. By fitting to experimental results, one can extract M_{sat} , m , and K . In the isotropic $K = 0$ limit, Eq. (1.5) reduces to the Langevin function,

$$M = M_{\text{sat}} L(x), \quad (1.6)$$

$$L(x) = \coth(x) - \frac{1}{x}, \quad (1.7)$$

with $x = mB/k_B T$. The rationale behind this approach is that the hybridization of the impurity levels with the host states produces broad resonances, thus a continuum description was judged more appropriate [10]. In the following we show that neither Brillouin nor Langevin function fits the results in an acceptable way.

1.3 Numerical renormalization group method

The Kondo model requires the use of non-perturbative techniques for correct description of its properties. The magnetization curves for the isotropic Kondo model (i.e. the $D = E = 0$ limit) can be calculated exactly using the Bethe-Ansatz technique [19]. In general, however, the problem needs to be addressed with numerical techniques, such as the NRG [20–22]. This approach consists of a discretization of the continuum of the conduction-band electrons into finite intervals with increasingly small width near the Fermi level, followed by a transformation into an effective one-dimensional tight-binding-chain model which is then diagonalized iteratively. After each iteration step, the exponentially growing number of many-particle levels is truncated to some relatively

small number; this is a good approximation since the matrix elements coupling excitations with very different characteristic energies are very small (this property is called the “energy-scale separation”).

All calculations presented in this work were performed using the “NRG Ljubljana” code with the discretization parameter $\Lambda = 3$ and the truncation cutoff set at $E_{\text{cutoff}} = 10\omega_N$. No z -averaging was used. Expectation values were calculated with the parameter $\tilde{\beta} = 1$. A test calculation for a decoupled $S = 1/2$ Kondo impurity has shown that the numerically calculated magnetization differs from the exact result as given by the corresponding Brillouin function by less than 0.001; this is thus an approximate upper bound for the error in all results presented in this work.

The magnetic moment is given by $\mathbf{m} = -\mu_B \langle \mathbf{S} \rangle$. At zero field, the model is symmetric with respect to the spin inversion $\mathbf{S} \rightarrow -\mathbf{S}$, thus $\mathbf{m} \equiv 0$. It is important to note that this is the case even in the presence of magnetic anisotropy of type (1.2).

1.4 Isotropic Kondo impurity

For a decoupled isotropic spin, the magnetization curve depends universally solely on $x = g\mu_B BS/k_B T$, a feature which is reproduced by NRG with very high numerical accuracy at all temperatures (this is a good test of the numerical procedure).

When the impurity couples to the host (i.e. $J \neq 0$), the magnetization curves depend on the ratio T/T_K , see Fig. 1.1. When the temperature is much higher than T_K , the magnetization curve strongly resembles the Brillouin function, although even for very high ratio $T/T_K = 72$ the discrepancies are in the few percent range and, in particular, the saturation to full spin polarization is (logarithmically) slow as the magnetic field is increased. For strong Kondo exchange interaction or, equivalently, for low temperature so that $T \ll T_K$, the magnetization curves are clearly very different from the free-paramagnetic-impurity results and a large magnetic field of the order of T_K is required to polarize the spin.

For large impurity spin the behavior remains similar, see Fig. 1.2. It is worth pointing out that even for relatively high $S = 5/2$, the continuous (classical) description in terms of the Langevin function differs significantly from the discrete (quantum) description in terms of the Brillouin function. Furthermore, the exchange coupling to the host does not make the field-dependence of the magnetization behave in a more “classical way” as might be erroneously expected since the impurity couples to a continuous (“decohering”) environment. A correct description of the impurity magnetization critically depends on the proper inclusion of the quantum many-particle effects, in particular the Kondo effect.

It is also instructive to compare the magnetization of impurities which couple to the host via antiferromagnetic (AFM) or via ferromagnetic (FM)

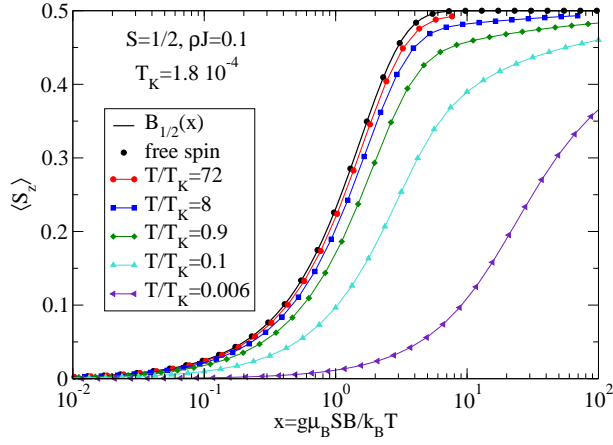


Fig. 1.1. Magnetization curves for an isotropic $S = 1/2$ Kondo impurity.

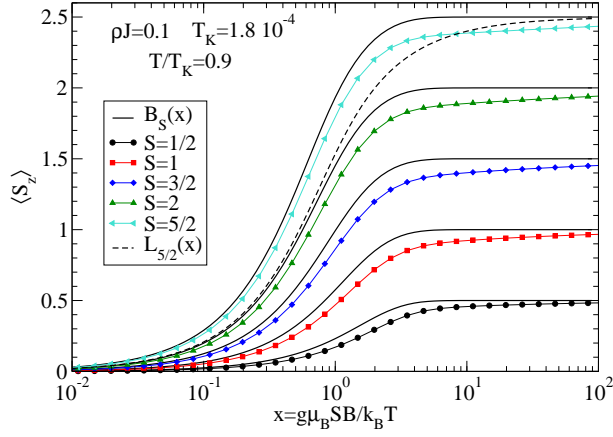


Fig. 1.2. Magnetization curves for isotropic spin- S Kondo impurities at a fixed exchange coupling and at constant temperature.

exchange coupling, Fig. 1.3. The host has a larger effect in the first case due to the presence of the Kondo effect, yet a deviation from free-spin Brillouin function is also found for FM coupling, in particular at large magnetic fields. The magnetization curves (scaled by $x \propto B/T$) in this case depend only little on the temperature, since no new dynamically-generated temperature scale emerges.

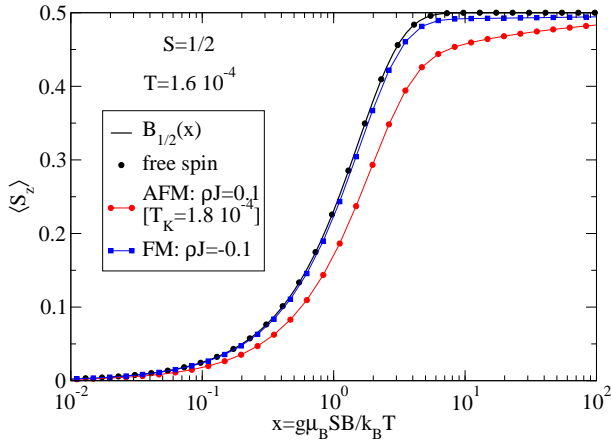


Fig. 1.3. Magnetization curves for an isotropic $S = 1/2$ Kondo impurity: comparison of antiferromagnetic and ferromagnetic exchange coupling to the host.

1.5 Anisotropic Kondo impurity

We now consider an anisotropic Kondo impurity in an external magnetic field. For Hamiltonian of a decoupled impurity ($J = 0$) with the anisotropic term of the form $DS_z^2 + E(S_x^2 - S_y^2)$, the vector $\langle \mathbf{S} \rangle$ will not point along the magnetic field \mathbf{B} , unless the magnetic field is applied along one of the principal axes (xyz). The expectation value $\langle \mathbf{S} \rangle$ can be easily derived for arbitrary spin S and field \mathbf{B} , however the expressions are lengthy.

As an illustration, we consider a spin-3/2 impurity with a planar anisotropy with $D = 0.01$ and transverse anisotropy $E/D = 0.1$. In this case, the low-energy $S_z = \pm 1/2$ multiplet behaves in many aspects as a $S = 1/2$ impurity [17], however the anisotropic nature of the system is fully revealed by its behavior in the magnetic field, see Fig. 1.4. For a decoupled impurity ($J = 0$), the behavior of $\langle S_z \rangle$ for a field along the z -axis is rather well described by the Brillouin function $B_{1/2}$. For a field along a transverse direction (x or y), the field dependence is more complex and the moment does not saturate, since the $S_z = \pm 3/2$ states start to play a role for fields approaching the scale of the magnetic anisotropy energy.

For weak coupling to the host ($\rho J = 0.05$), the magnetization curves are only moderately modified since the Kondo temperature is much lower than the experimental temperature, Fig. 1.4. For stronger coupling ($\rho J = 0.1$) such that the Kondo temperature is higher than the experimental temperature (here the Kondo temperature of the effective spin-1/2 Kondo effect [17, 18] is $T_K(S = 1/2) = 9 \times 10^{-4}$, therefore $T/T_K = 0.01$), the magnetization curves are strongly affected and the moment becomes well developed only for magnetic field much higher than T_K , as expected.

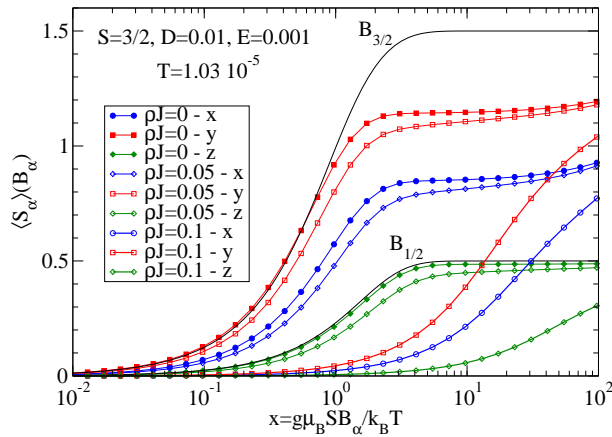


Fig. 1.4. Magnetization curves for an anisotropic $S = 3/2$ Kondo impurity with both longitudinal and transverse magnetic anisotropy.

1.6 Effect of the hybridization

When the effect of the hybridization is taken into account by describing the impurity in terms of the Anderson impurity model, the impurity local moment defined as $\langle \mathbf{S}^2 \rangle$ will be reduced due to charge fluctuations. For this reason, at moderately high magnetic fields the impurity spin polarization will not saturate at $1/2$, but at some reduced value (for simplicity, we discuss here the non-degenerate single-orbital model at half-filling, i.e. at the particle-hole symmetric point). In addition, as in the previously discussed case of the Kondo impurity, at low temperatures the Kondo effect will be at play, thus there will be further deviation from the free-spin behavior. Both features are well illustrated in Fig. 1.5, where we consider an Anderson impurity with a very high $U/\pi\Gamma$ ratio of 12.7, so that the system is well in the Kondo limit. The local moment fraction $f_{\text{lm}} = \langle n - 2n_\uparrow n_\downarrow \rangle = \langle 2n - n^2 \rangle$ is then approximately 0.97 at low temperatures and low magnetic field. Accordingly, we find that the spin polarization saturates at approximately $0.97/2 = 0.485$, rather than $1/2$.

For low $U/\pi\Gamma$ ratio, charge fluctuations become larger and the Kondo temperature T_K eventually increases to the scale of U , in which case there is no Kondo effect in the usual sense (conventionally, the limit for the existence of the local moment is considered to be $U/\pi\Gamma = 1$, the point where the Hartree-Fock approximation breaks down, although the transition is in fact continuous and in the correct solution nothing particular happens at the said point). In the $U/\pi\Gamma \ll 1$ limit, the only relevant scales are bare U and Γ . The magnetization is then low as long as $B \lesssim U$, i.e. it is not possible to polarize the impurity using laboratory magnetic fields. The impurity is then non-magnetic for all practical purposes. Similar deviations from the Kondo-limit behavior

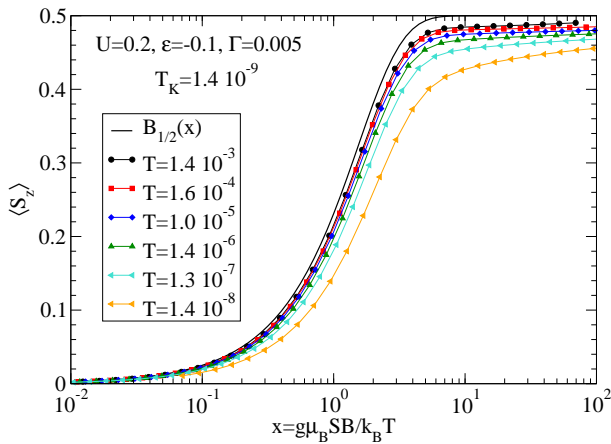


Fig. 1.5. Magnetization curves for the Anderson impurity model with parameters chosen so that the system is in the Kondo regime at low enough temperatures.

may be found in the valence fluctuation regime when the impurity orbital is away from half-filling, i.e. for $|\epsilon_d| \gtrsim \Gamma$.

We thus conclude that in all parameter ranges, the magnetization of an Anderson impurity cannot be described by the Brillouin function nor, in fact, by the Langevin function as it is sometimes done. This result clearly carries over to the multi-orbital Anderson model and it is general. It is thus expected that fitting XMCD results by Brillouin or Langevin function may lead to significant systematic errors. The only regime where reasonably good curve fitting by a modified (rescaled and shifted) Brillouin function can be performed is in the strong Kondo limit (large $U/\pi\Gamma$ ratio, i.e. for low charge fluctuations, when the Anderson model maps onto an effective Kondo model by the Schrieffer-Wolff transformation) for temperature well above the Kondo temperature, as illustrated in Fig. 1.6.

1.7 Conclusion

It was shown that the magnetization curves for magnetic impurities adsorbed on a metallic substrate strongly depend on the strength of the exchange coupling with the substrate conduction-band electrons. If the Kondo effect is well developed (i.e. if $T \ll T_K$), the magnetization is strongly suppressed unless the magnetic field becomes comparable to the scale of the Kondo temperature. It is important to note, however, that even for T/T_K as small as 0.1, the moment is not fully Kondo screened and that at moderate magnetic fields $g\mu_B SB \sim k_B T$ the magnetization is still sizeable. Only for weak exchange coupling (i.e. $T_K \ll T$) are the magnetization curves qualitatively compa-

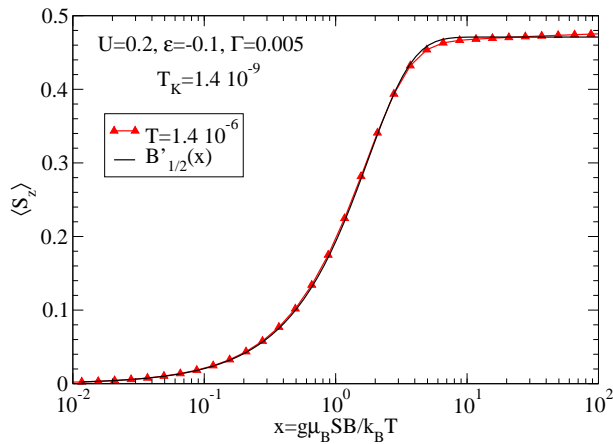


Fig. 1.6. Magnetization curve for the Anderson impurity model for $T \gg T_K$ fitted using a shifted and rescaled Brillouin function $B'(x) = aB(bx)$.

rable to Brillouin functions, although quantitative deviations are still very pronounced even for T/T_K as large as 10.

We conclude by noting that in principle it is possible to extract all experimental parameters (spin S , Kondo temperature T_K , magnetic anisotropies D and E) from known magnetization curves $\langle S_z \rangle(B)$, although this would constitute a difficult non-linear curve fitting problem involving repeated numerical calculations of the magnetization curves using NRG. Nevertheless, this approach would be more reliable than the extraction of anisotropy parameters by fitting XMCD results using the magnetization curves obtained from classical spin models (i.e. in the $S \rightarrow \infty$ limit). The results presented in this work should serve as a caveat against such over-simplified parameter extraction procedures.

References

1. H. Brune and P. Gambardella. Magnetism of individual atoms adsorbed on surfaces. *Surf. Sci.*, 602:1812, 2009.
2. A. C. Hewson. *The Kondo Problem to Heavy-Fermions*. Cambridge University Press, Cambridge, 1993.
3. Alexander F. Otte, Markus Ternes, Kirsten von Bergmann, Sebastian Loth, Harald Brune, Christopher P. Lutz, Cyrus F. Hirjibehedin, and Andreas J. Heinrich. The role of magnetic anisotropy in the kondo effect. *Nature Physics*, 4:847, 2008.
4. M. Ternes, A. J. Heinrich, and W. D. Schneider. Spectroscopic manifestations of the kondo effect on single adatoms. *J. Phys.: Condens. Matter*, 21:053001, 2009.
5. Cyrus F. Hirjibehedin, Chiun-Yuan Lin, Alexander F. Otte, Markus Ternes, Christopher P. Lutz, Barbara A. Jones, and Andreas J. Heinrich. Large magnetic

- anisotropy of a single spin embedded in a surface molecular network. *Science*, 317:1199, 2007.
6. Y. Yayon, V. W. Brar, L. Senapati, S. C. Erwin, and M. F. Crommie. Observing spin polarization of individual magnetic adatoms. *Phys. Rev. Lett.*, 99:067202, 2007.
 7. F. Meier, L. H. Zhou, J. Wiebe, and R. Wiesendanger. Revealing magnetic interactions from single-atom magnetization curves. *Science*, 320:82, 2008.
 8. T. Balashov, T. Schuh, A. F. Takacs, A. Ernst, S. Ostanin, J. Henk, I. Mertig, P. Bruno, T. Miyamachi, S. Suga, and W. Wulfhekel. Magnetic anisotropy and magnetization dynamics of individual atoms and clusters of fe and co on pt(111). *Phys. Rev. Lett.*, 102:257203, 2009.
 9. P. Gambardella, S. S. Dhesi, S. Gardonio, C. Grazioli, P. Ohresser, and C. Carbone. Localized magnetic states of fe, co, and ni impurities on alkali metal films. *Phys. Rev. Lett.*, 88:047202, 2002.
 10. P. Gambardella, S. Rusponi, M. Veronese, S. S. Dhesi, C. Grazioli, A. Dallmeyer, I. Cabria, R. Zeller, P. H. Dederichs, K. Kern, C. Carbone, and H. Brune. Giant magnetic anisotropy of single cobalt atoms and nanoparticles. *Science*, 300:1130, 2003.
 11. P. Gambardella, S. Stepanow, A. Dmitriev, J. Honolka, F. M. F. de Groot, M. Lingenfelder, S. Sen Gupta, D. D. Sarma, P. Bencok, S. Stanescu, S. Clair, S. Pons, N. Lin, A. P. Seitsonen, H. Brune, J. V. Barth, and K. Kern. Supramolecular control of the magnetic anisotropy in two-dimensional high-spin fe arrays at a metal interface. *Nature Materials*, 8:189, 2009.
 12. G. Schütz, W. Wagner, W. Wilhelm, P. Kienle, R. Zeller, R. Frahm, and G. Materlik. Absorption of circularly polarized x-rays in iron. *Phys. Rev. Lett.*, 58:737, 1987.
 13. C. T. Chen, F. Sette, Y. Ma, and S. Modesti. Soft-x-ray magnetic circular dichroism at the l_{2,3} edges of nickel. *Phys. Rev. B*, 42:7262, 1990.
 14. B. T. Thole, P. Carra, F. Sette, and G. van der Laan. X-ray circular dichroism as a probe of orbital magnetization. *Phys. Rev. Lett.*, 68:1943, 1992.
 15. P. Carra, B. T. Thole, M. Altarelli, and X. Wang. X-ray circular dichroism and local magnetic fields. *Phys. Rev. Lett.*, 70:694, 1993.
 16. C. T. Chen, Y. U. Idzerda, H.-J. Lin, N. V. Smith, G. Meigs, E. Chaban, G. H. Ho, E. Pellegrin, and F. Sette. Experimental confirmation of the x-ray magnetic circular dichroism sum rules for iron and cobalt. *Phys. Rev. Lett.*, 75:152, 1995.
 17. Rok Žitko, Robert Peters, and Thomas Pruschke. Properties of anisotropic magnetic impurities on surfaces. *Phys. Rev. B*, 78:224404, 2008.
 18. R. Žitko, Robert Peters, and Thomas Pruschke. Splitting of the kondo resonance in anisotropic magnetic impurities on surfaces. *New J. Phys.*, 11:053003, 2009.
 19. N. Andrei, K. Furuya, and J. H. Lowenstein. Solution of the kondo problem. *Rev. Mod. Phys.*, 55:331, 1983.
 20. K. G. Wilson. The renormalization group: Critical phenomena and the kondo problem. *Rev. Mod. Phys.*, 47:773, 1975.
 21. H. R. Krishna-murthy, J. W. Wilkins, and K. G. Wilson. Renormalization-group approach to the anderson model of dilute magnetic alloys. i. static properties for the symmetric case. *Phys. Rev. B*, 21:1003, 1980.
 22. Ralf Bulla, Theo Costi, and Thomas Pruschke. The numerical renormalization group method for quantum impurity systems. *Rev. Mod. Phys.*, 80:395, 2008.